

Supporting information

Transformation of homobimetallic MOFs to nickel-cobalt phosphide/nitrogen-doped carbon polyhedral nanocages for efficient oxygen evolution electrocatalysts

Xueping Zhang,^{a,b} Liang Huang,^{a,c} Qingqing Wang^a and Shaojun Dong^{*,a,b}

^aState Key Laboratory of Electroanalytical Chemistry, Changchun Institute of Applied Chemistry, Chinese Academy of Sciences, Changchun 130022, P. R. China

^bUniversity of Chinese Academy of Sciences, Beijing 100049, P. R. China

^cUniversity of Science and Technology of China, Hefei, Anhui 230026, P. R. China

*E-mail: dongsj@ciac.ac.cn

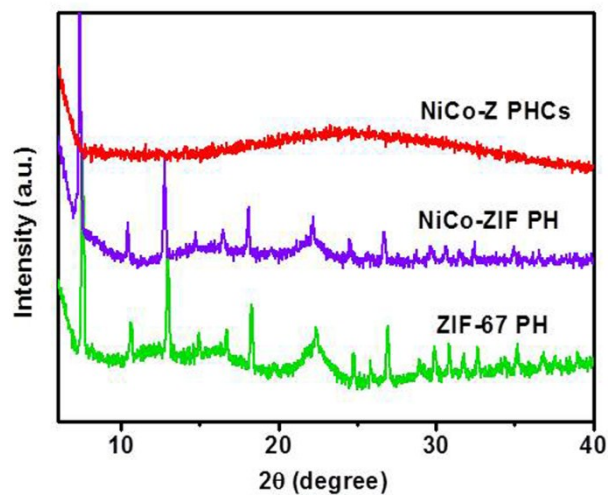


Fig. S1 XRD patterns of NiCo-Z PHCs, NiCo-ZIF PH, and ZIF-67 PH.



Fig. S2 The picture of solid samples of NiCo-ZIF PH, NiCo-Z PHCs, and NiCoP/NC PHCs.

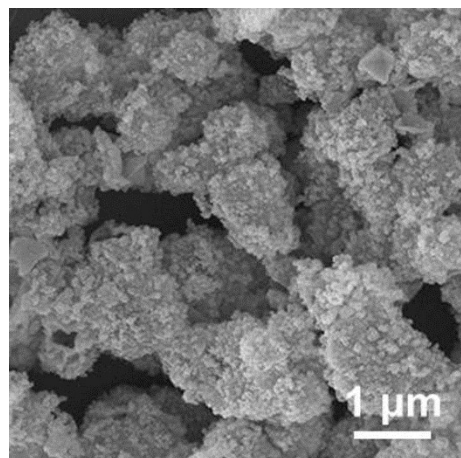


Fig. S3 SEM image of the scale-up synthesis of NiCo-Z PHCs by using 200 mg of NiCo-ZIF PH and 100 mL of methanol solution containing 500 mg of tannic acid.

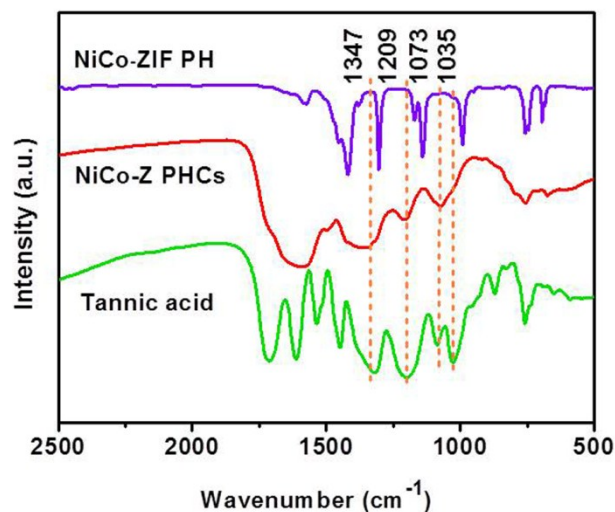


Fig. S4 FT-IR spectra of NiCo-ZIF PH, NiCo-Z PHCs, and tannic acid.

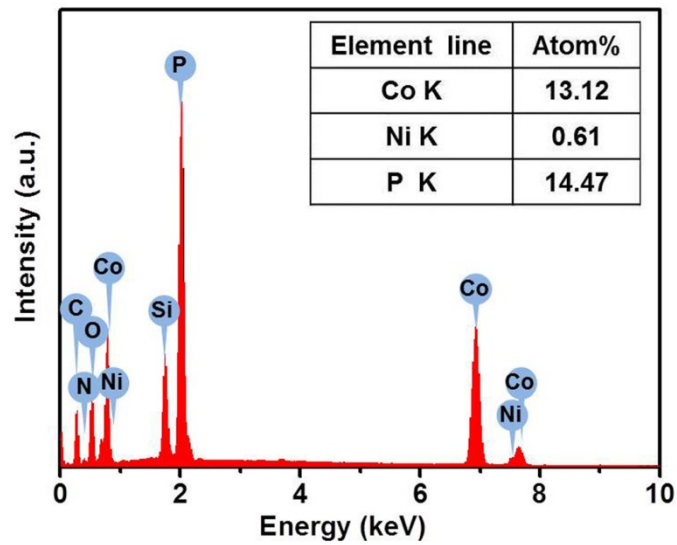


Fig. S5 EDX spectrum of NiCoP/NC PHCs.

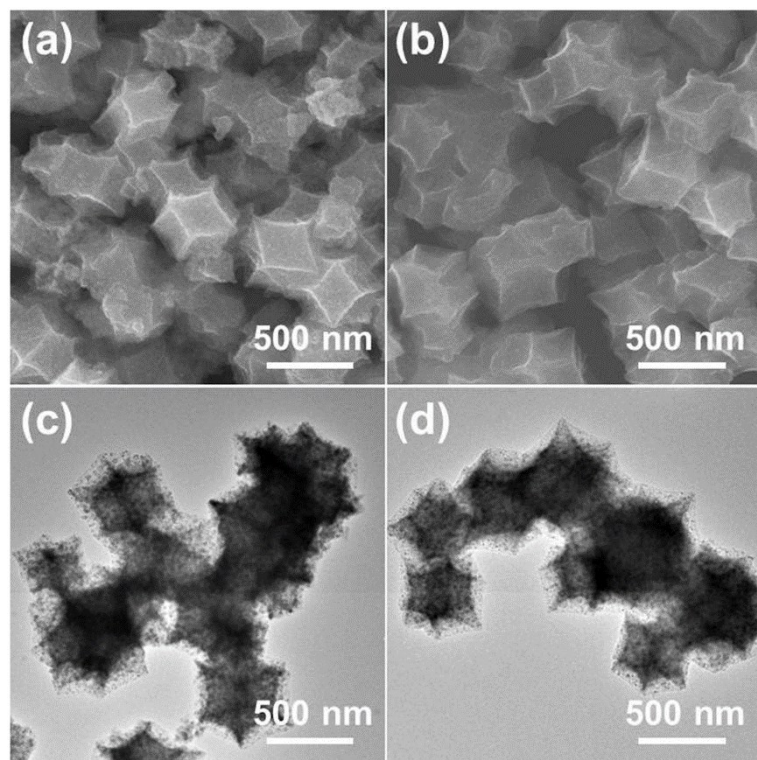


Fig. S6 SEM and TEM images of (a, c) NiCoP/NC PH and (b, d) CoP/NC PH.

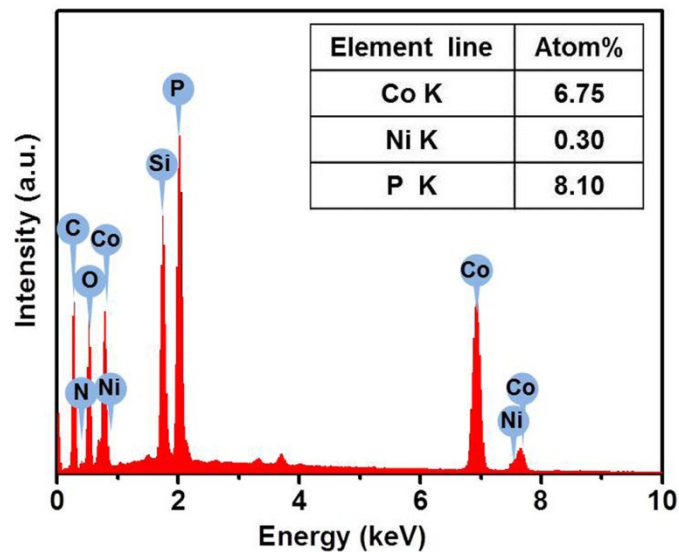


Fig. S7 EDX spectrum of NiCoP/NC PH.

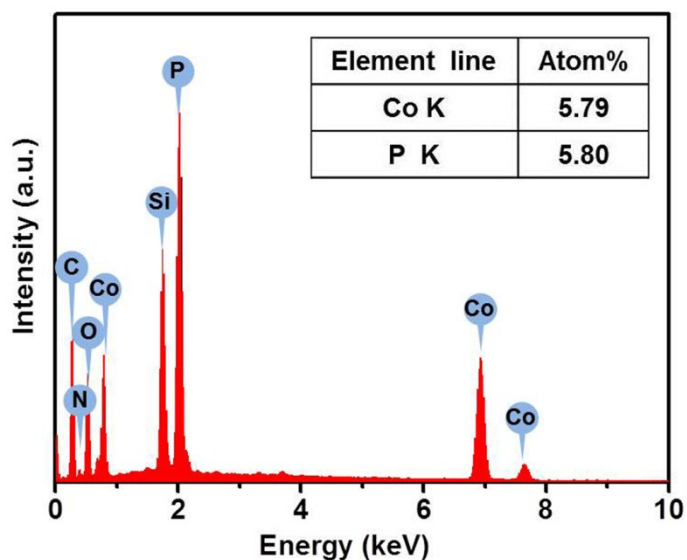


Fig. S8 EDX spectrum of CoP/NC PH.

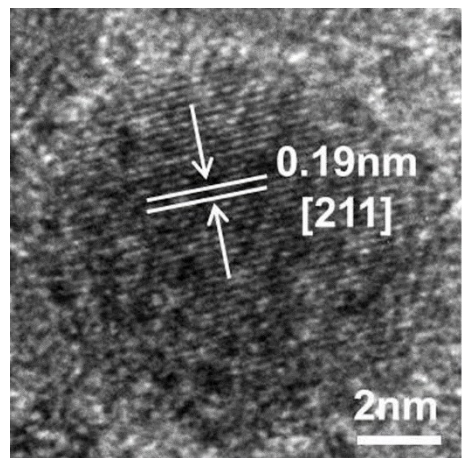


Fig. S9 HR-TEM images of NiCoP/NC PHCs.

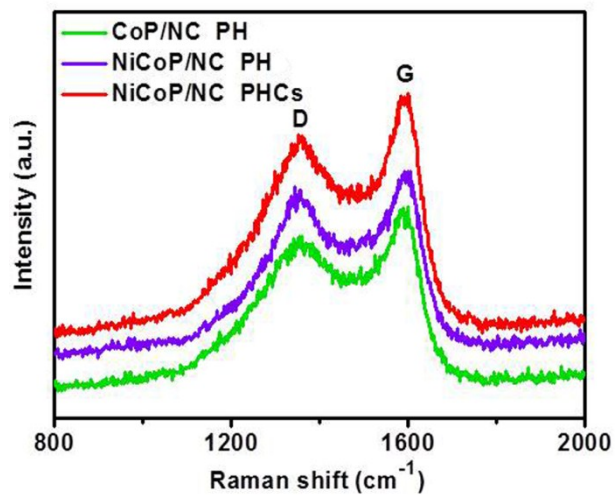


Fig. S10 Raman spectra of NiCoP/NC PHCs, NiCoP/NC PH and CoP/NC PH.

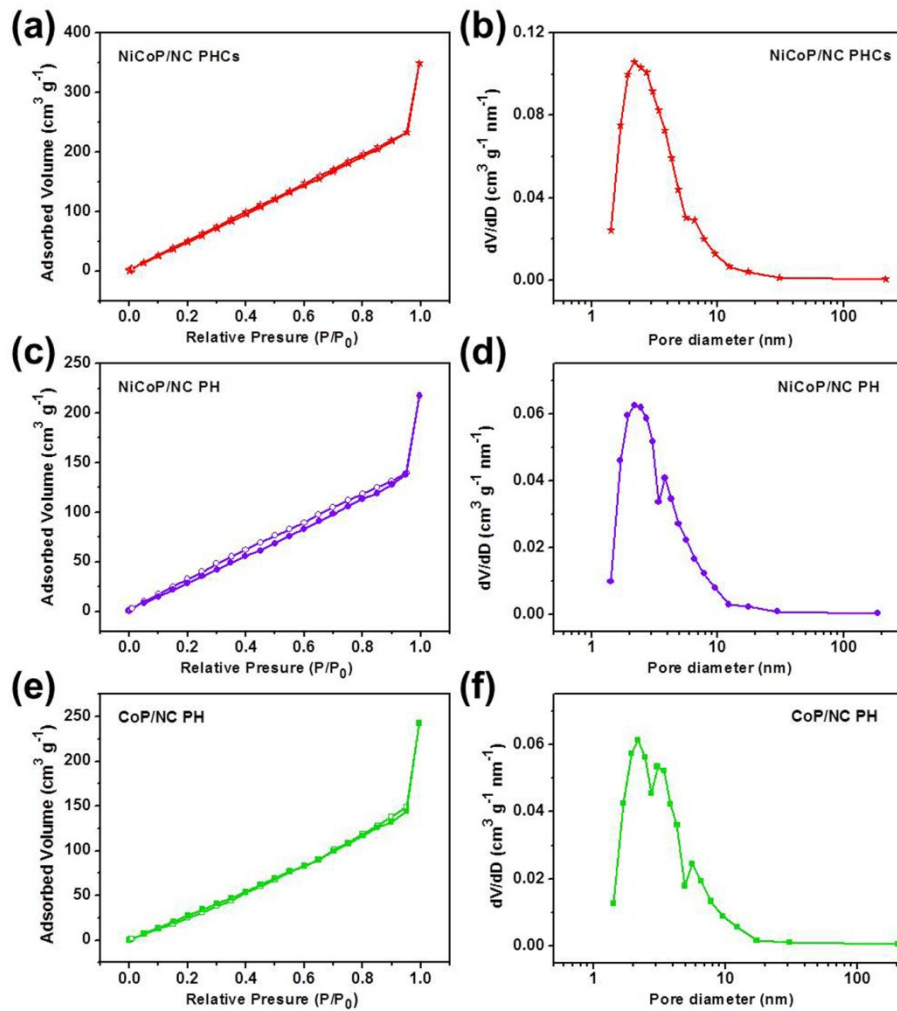


Fig. S11 Nitrogen adsorption and desorption isotherms and BJH pore distribution of (a, b) NiCoP/NC PHCs, (c, d) NiCoP/NC PH and (e, f) CoP/NC PH.

Table S1. The surface area and pore volume of different samples

Sample	S_{BET} ($\text{m}^2 \text{ g}^{-1}$)	V_{pore} ($\text{cm}^3 \text{ g}^{-1}$)	D_{BJH} (nm)
NiCoP/NC PHCs	384.6	0.662	2.188
NiCoP/NC PH	235.0	0.406	2.191
CoP/NC PH	219.7	0.447	2.190

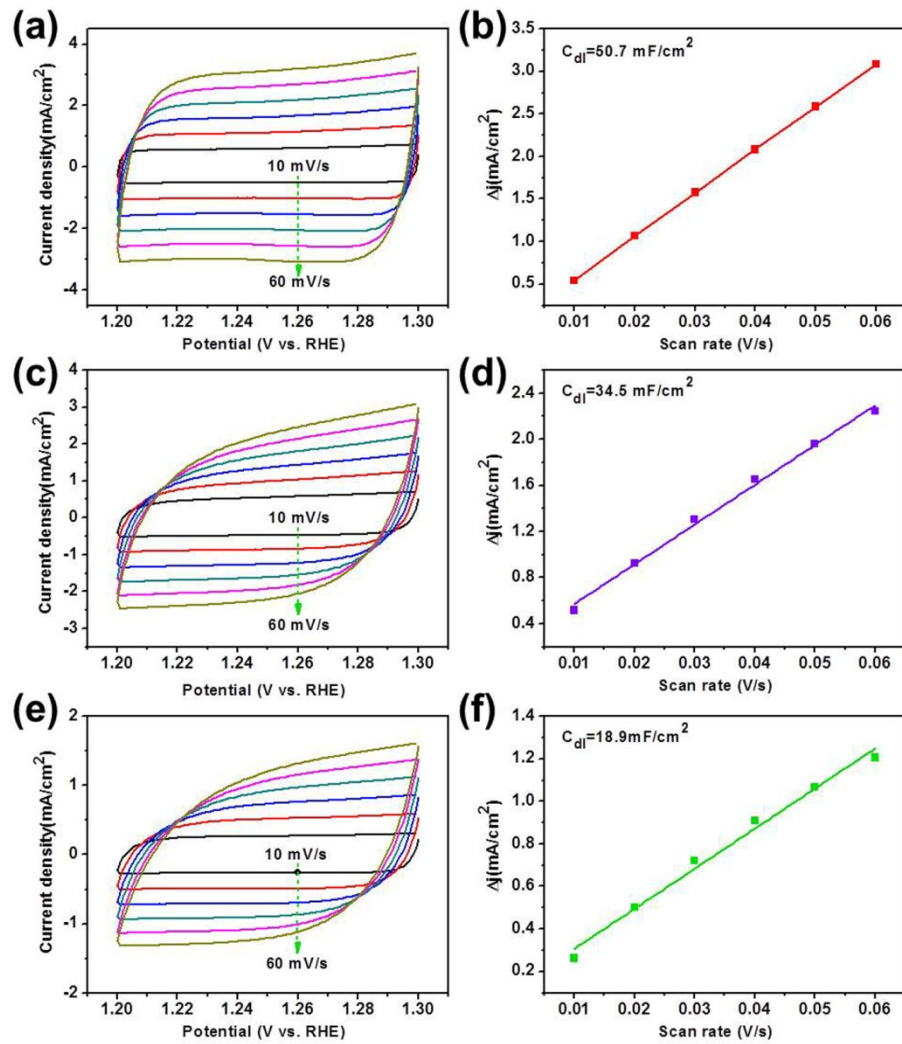


Fig. S12 CV curves of (a) NiCoP/NC PHCs, (c) NiCoP/NC PH and (e) CoP/NC PH in the double layer region at scan rates of 10-60 mV s⁻¹ in 1.0 M KOH. (b), (d), and (f) current density as a function of scan rate derived from (a), (c) and (e), respectively.

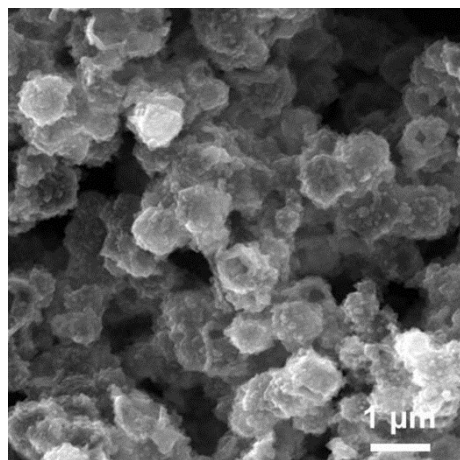


Fig. S13 SEM image of NiCoP/NC PHCs after long-term stability test.

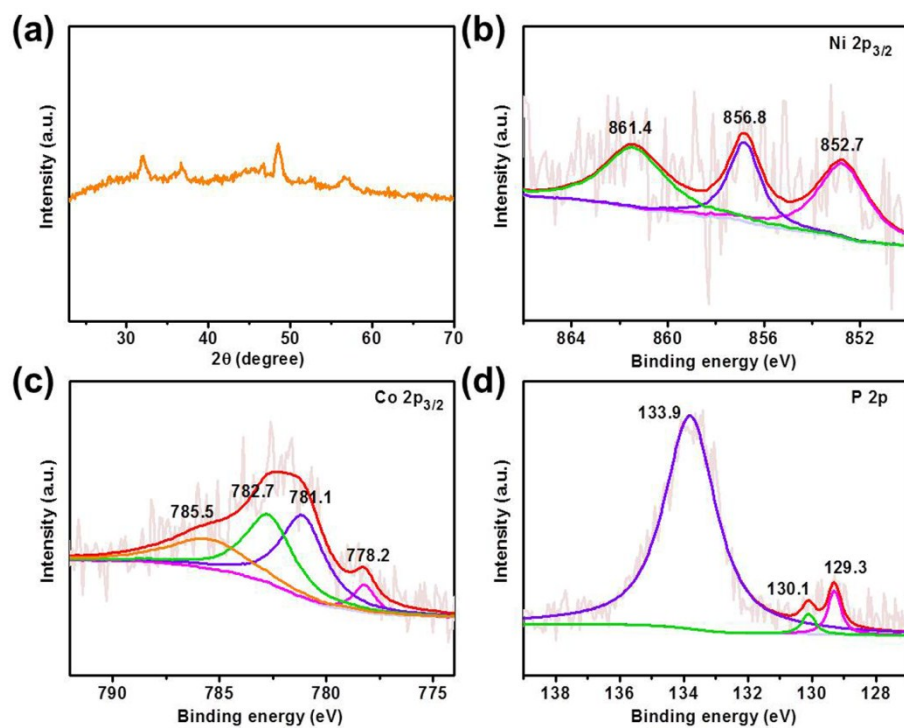


Fig. S14 (a) XRD pattern of NiCoP/NC PHCs, and the high resolution XPS spectra of (b) Ni 2p_{3/2}, (c) Co 2p_{3/2}, and (d) P 2p after long-term stability test.

Table S2. Comparison of the OER electrocatalytic performance for different catalysts.

Catalysts	Overpotential (mV) at 10 mA/cm ²	Reference
NiCoP/NC PHCs	297	This work
NiCoP/C nanoboxes	330	<i>Angew. Chem. Int. Ed.</i> 2016 , <i>55</i> , 10381
MnCoP nanoparticles	330	<i>J. Am. Chem. Soc.</i> 2016 , <i>138</i> , 4006
NiCoP microspheres	340	<i>Adv. Mater. Interfaces</i> 2016 , <i>3</i> , 1500454
Co-Fe-P nanoparticles	280	<i>Angew. Chem. Int. Ed.</i> 2015 , <i>54</i> , 9642
CoP hollow polyhedron	400	<i>ACS Appl. Mater. Interfaces</i> 2016 , <i>8</i> , 2158
Co-P/NC nanopolyhedrons	354	<i>Chem. Mater.</i> 2015 , <i>27</i> , 7636
Ni ₂ P nanoparticles	290	<i>Energy Environ. Sci.</i> 2015 , <i>8</i> , 2347
Co-NC@CoP-NC	330	<i>J. Mater. Chem. A</i> , 2016 , <i>4</i> , 15836
Co ₂ P/Co-foil	319	<i>J. Mater. Chem. A</i> , 2017 , <i>5</i> , 10561
Co-P-foam	300	<i>J. Mater. Chem. A</i> , 2016 , <i>4</i> ,

Note: All the overpotentials were measured in 1.0 M KOH.